





Wideband ultrathin and polarization insensitive metamaterial absorber for Ku-band applications

A. Samy Saadeldin¹ , Amr M. Sayed¹, Adnan M. Amr¹, Menna O. Sayed¹, Mohamed Farhat O. Hameed^{2,3,4}, and S. S. A. Obayya^{5,6,*} 

¹ Electronics and Communication Engineering Department, Akhbar Elyom Academy, 6th of October City, Giza, Egypt

² Nanotechnology and Nanoelectronics Engineering Program, Zewail City of Science, Technology and Innovation, October Gardens, 6th of October City, Giza 12588, Egypt

³ Center of Nanotechnology, Zewail City of Science, Technology and Innovation, October Gardens, 6th of October City, Giza 12588, Egypt

⁴ Mathematics and Engineering Physics Department, Faculty of Engineering, University of Mansoura, Mansoura 35516, Egypt

⁵ Center for Photonics and Smart Materials, Zewail City of Science, Technology and Innovation, October Gardens, 6th of October City, Giza 12588, Egypt

⁶ Department of Electronics and Communication Engineering, Faculty of Engineering, University of Mansoura, Mansoura 35516, Egypt

Received: 22 December 2022

Accepted: 12 August 2023

© The Author(s), 2023

ABSTRACT

In this paper, wideband, and ultrathin metamaterial absorber is proposed, analyzed and fabricated for Ku-band applications. The reported absorber has a nearly perfect absorptivity above 90% covering the entire Ku band (12–20 GHz) at normal incidence for both transverse electric and transverse magnetic polarization. This is due to the supported electric and magnetic resonances simultaneously. Consequently, the effective permittivity and permeability can be designed to obtain impedance matching with free space. This leads to the absorption of the entire incident energy in the metamaterial absorber. The suggested structure also shows a good absorption response (above 80%) under oblique incidence (from 0 to 50°). Therefore, the proposed absorber represents a good potential for Ku-band applications.

1 Introduction

Engineered metamaterials have unique properties that are beyond what can be found in nature ($\epsilon < \epsilon_0$ and $\mu < \mu_0$) [1]. Therefore, metamaterials have attracted the attention during the last years for different applications such as super lenses [2], invisibility cloaking [3], polarization rotation [4], energy harvesting [5], perfect absorbers [6], and antennas [7]. Electromagnetic

perfect metamaterial absorber (PMMA) is one of the most encouraging applications with compact size, lightweight, and wideband operation. The metamaterial absorber can be used in many applications such as; stealth technology [8], specific absorption rate (SAR) reduction [9], internet of things (IoT) [10], and sensing [11]. In this context, Xiong et al. [12] presented an ultrathin broadband absorber based on periodic array of loop-dielectric multilayered structure with

Address correspondence to E-mail: sobayya@zewailcity.edu.eg

higher absorption than 90% in the frequency range of 8.37–21 GHz. In [13], a microwave ultra-broadband polarization-independent metamaterial absorber was fabricated using periodic array of metal-dielectric multilayered quadrangular frustum pyramids with absorption above 90% in the frequency range of 7.8–14.7 GHz. Nguyen et al. [14], proposed a broadband metamaterial (MM) absorber using eight-resistive-arm (ERA) cell with absorption ratio higher than 90% in the range of 8.2–13.4 GHz. In [15], a wideband and polarization-/wide-angle insensitive metamaterial absorber has been reported using a symmetric structure associated with surface mount resistors with absorption above 80% within 8–18 GHz. Araújo et al. [16] introduced an ultrathin and ultra-wideband metamaterial absorber with periodically-arranged metallic square spirals. It has been shown that an absorptivity of more than 90% was achieved from 11.4 to 20.0 GHz [16]. Jagtap et al. [17] investigated the ferro-nano-carbon split ring resonators in the X-band (8–12 GHz) region. Such split ring resonators acted as a bianisotropic left-handed material with a cloak-like response between 8.5 and 10 GHz. Further, a triple band microwave metamaterial absorber was presented by Bellal et al. [18] for electromagnetic interference shielding and stealth applications inspired by double E-shaped symmetric split ring resonators metamaterial in C and X band. Such a design has absorptivity of 99% at resonance frequencies. In [19], broadband metamaterial absorber with optically transparent property was proposed for solving the electromagnetic pollution problem at gigahertz. An absorption over 90% at frequency range of 6–17.6 GHz was obtained.

It is worth noting that there are many approaches to overcome the narrowband response of the PMMA. The first technique is to use multilayered structure [12], while the second approach is to combine lumped elements into the metamaterial absorber [15]. Further, many resonating structures can be used in the same unit cell [14]. Additionally, redistribution of charges can be used to create more electric and magnetic dipoles which broadens the absorption bandwidth. This can be achieved by splitting the resonator structure into separated sections [16].

In this paper, wideband ultrathin metamaterial absorber is designed, fabricated and characterized in Ku-band. The reported structure has a compact size with unit cell dimension of 3.7 mm × 3.7 mm (i.e. 0.148 λ at lowest frequency). The suggested metamaterial absorber is numerically studied by using the

commercial computer simulation technology (CST) Microwave Studio software with a frequency-domain solver [20]. Then a prototype of PMMA is fabricated and measured to ensure a good agreement between the measured and simulated results. The reported absorber shows perfect absorptivity greater than 90% for the entire Ku-band and part of k-band. Also, the proposed PMMA is polarization insensitive. Further, the suggested PMMA has a good stability for the variation of the incident angle (up to 50°). It is worth noting that most of the previously reported metamaterial absorber based on multilayered structure and/or using lumped element with minimum unit cell dimensions of 9.7 × 9.7 × 2.5 mm with complex structures [15, 21, 22]. Therefore, the proposed PMMA has advantages in terms of compactness, high absorption and polarization insensitivity with simple design. It is worth noting that the proposed perfect metamaterial absorber has many future prospects. It can improve the radar performance and prove concealment against others' radar systems that was utilized as a military technique [23]. Further, radar cross section (RCS) can be reduced using metamaterial absorber to decrease the radar echo where the objects can have a greater element of stealth [24]. Additionally, it can be also used for decreasing the sidelobe radiation of antennas with reduced undesirable radiation [25]. Furthermore, the electromagnetic interference can be minimized by absorbing spurious electromagnetic radiation. Along with preventing health risks due to exposure of specific electromagnetic radiation at particular frequencies, it is also useful for wireless communication. [26].

2 Design considerations

Figure 1a and b show cross section and 3D configuration of the proposed PMMA. The reported absorber consists of L-shaped copper resonators and continuous copper ground plane separated by dielectric spacer. The top and bottom layers have thickness of 0.035 mm. The copper is modelled with a frequency independent conductivity $\sigma = 5.96 \times 10^7$ S/m. However, the dielectric substrate is made by low cost FR-4 with a thickness (h) of 1.6 mm (0.064 λ at lowest frequency). The FR-4 material has a relative dielectric constant of 4.3, and a loss tangent of 0.025 [15]. The separation (d) and the L-shaped resonators of the top layer (Fig. 1b) lead to wideband absorption response instead of multiple peaks as a result of each resonator [16, 27]. The separation (d) has a direct

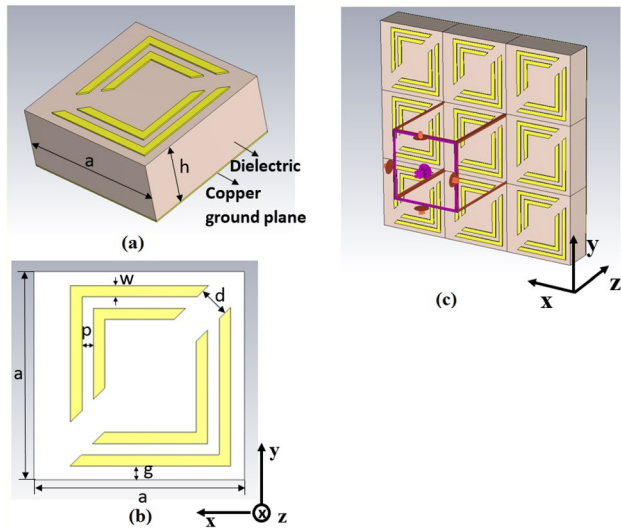


Fig. 1 **a** 3D perspective view, **b** cross section of the L-shaped resonators and **c** the applied boundary conditions

impact on the absorption response due to the redistribution of charges with more electric and magnetic dipoles [16]. The commercial computer simulation technology (CST) Microwave Studio software with a frequency-domain solver is used to analyze the suggested design. In this study, periodic boundary conditions are used around the unit cell in the *x*- and *y*- directions, while open boundary condition (Perfect matched layer) is set in the *z*-direction as shown in Fig. 1c. The incident wave is propagating along *z* direction. The tetrahedral mesh is applied in the model with an accuracy of 10^{-4} with minimum element quality of 0.02684 and total number of elements of 35,164.

The absorption (*A*) of the PMMA can be calculated through reflection and transmission coefficients according to:

$$A = 1 - R - T = 1 - S_{11}^2 - S_{21}^2 \tag{1}$$

where S_{11} and S_{21} represent the reflection coefficient and transmission coefficient, respectively. It is worth noting that there is no transmission in our case because of the bottom copper layer with thickness of 0.035 mm which acts as a perfect reflector, i.e. $S_{21} = 0$. Therefore, the absorption in our case can be determined by Eq. (2).

$$A = 1 - S_{11}^2 \tag{2}$$

The metamaterial is an engineered material that possess unique properties with ($\epsilon < \epsilon_0$ and $\mu < \mu_0$). In this study, the effective permittivity (ϵ_{eff}), effective permeability (μ_{eff}), and relative impedance (Z_r) are obtained through the S-parameters [16] by Eqs. (3), (4), and (5). This approach is convenient for the suggested absorber, once the transmission coefficient S_{21} is not needed due to the copper ground plate. These calculations can help understand the absorption mechanism.

$$\epsilon_{eff} = 1 + \frac{2j}{K_0 h} \left(\frac{1 - S_{11}}{1 + S_{11}} \right) \tag{3}$$

$$\mu_{eff} = 1 + \frac{2j}{K_0 h} \left(\frac{1 + S_{11}}{1 - S_{11}} \right) \tag{4}$$

$$Z_r = \sqrt{\frac{(1 + S_{11})^2 - S_{21}^2}{(1 - S_{11})^2 - S_{21}^2}} = \frac{1 + S_{11}}{1 - S_{11}} \tag{5}$$

where K_0 is the free space wave number, and h is the substrate thickness.

Figure 2a and b show the real and imaginary parts of the effective permittivity and effective permeability, respectively of the suggested PMMA. It may be seen from Fig. 2a and b that the value of both effective permittivity and effective permeability are approximately equal through the absorption frequency band. Therefore, the absorption response is due to the presence of both electric and magnetic resonance simultaneously.

It may be seen from Fig. 2a that the imaginary part of the dielectric constant of PMMA is negative at 11–13 GHz. The negative sign can be referred to the transformation of the magnetic energy into the electric energy [28] which is called magnetoelectric coupling as reported by Zhang et al. [28]. However, the total energy loss is still positive. Further, for metamaterial, if the magnetoelectric coupling occurs, the negative imaginary part of the dielectric constant can be classified as an intrinsic character rather than non-physical one. It is worth noting that there are other wideband perfect metamaterial absorbers that have negative imaginary part of the dielectric constant through the studied frequency band [29, 30]–[31]. It is worth noting that the dielectric constant and permeability spectra shown in Fig. 2a and b are calculated from the S-parameters using the FEM [20]. Further, the dielectric constant and permeability spectra show a good agreement with the Lorentz model [32], 33. This is an evident for the presence of the electron

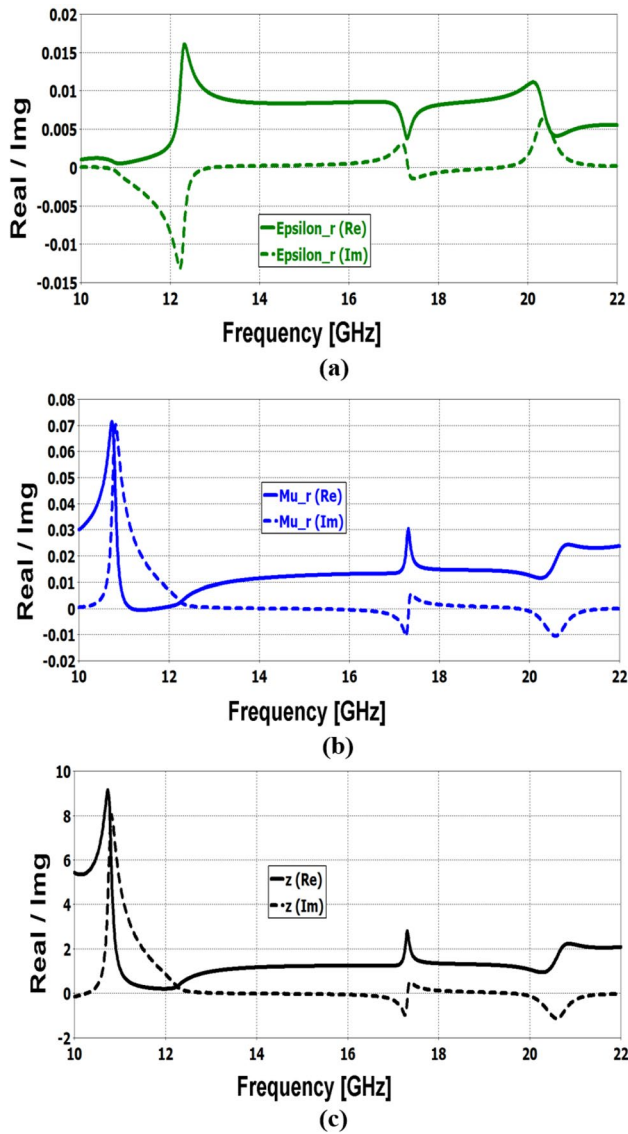


Fig. 2 a Effective permittivity, b effective permittivity, and c relative impedance of the reported metamaterial absorber

and current oscillations with a resonance response. Figure 2c shows the real and imaginary parts of the impedance of the suggested PMMA normalized to the impedance of the free space (i.e. relative impedance). It may be observed from Fig. 2c that the real part equals to unity while the imaginary part equals to zero. This means that the impedance matching (between metamaterial absorber impedance and free space impedance, $Z_0 = 377 + j0 \Omega$) is obtained which leads to a smaller amount of reflected power from the structure. Through the frequency range (12–20 GHz), a damping oscillation is obtained due to the resistive behavior of the metamaterial impedance during the

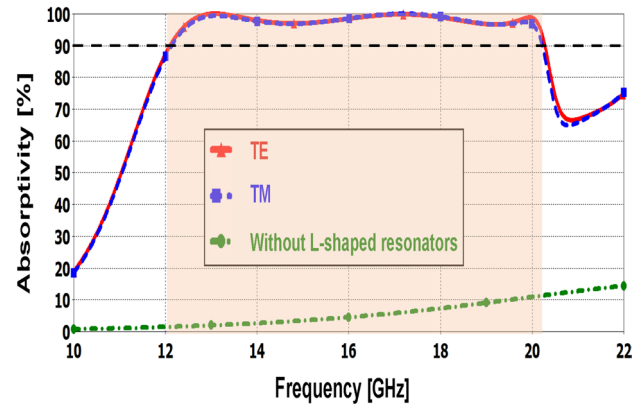


Fig. 3 The absorption response of the proposed PMMA at normal incidence for both TE and TM, and the absorption response without L-shaped resonators

microwave oscillation. Additionally, the transmission equals to zero in our case due to the copper ground plane. Hence maximum absorptivity occurs at the desired frequency band.

3 Results and discussion

The design geometrical parameters shown in Fig. 1 are initially taken as $h = 1.6 \text{ mm}$, $g = 0.3 \text{ mm}$, $a = 3.7 \text{ mm}$, $p = 0.2 \text{ mm}$, $w = 0.2 \text{ mm}$ and $d = 0.5 \text{ mm}$, some of these parameters are taken according to the fabrication feasibility. Figure 3 shows the simulated absorption response of the suggested PMMA for both TE and TM polarizations at normal incidence.

It may be seen that the proposed PMMA has an absorption response with absorptivity above 90% in a wide frequency band from 12 to 20.2 GHz covering the entire Ku-band and part of K-band. Also, the reported PMMA can be regarded as polarization insensitive absorber due to similar absorption response for both TE and TM polarizations. Figure 3 also shows the absorptivity of the proposed design without the L-shaped resonators (dash-dot line) and with presence of the copper ground plane. It can be seen that the maximum absorptivity without the proposed L-shaped resonators is equal to 14% at 22 GHz. Therefore, the L-shaped resonators play important role in the absorption response of the reported design. Figure 4 shows the effect of the incident angle on the absorption response for both TE and TM polarizations. The suggested PMMA shows a good stability

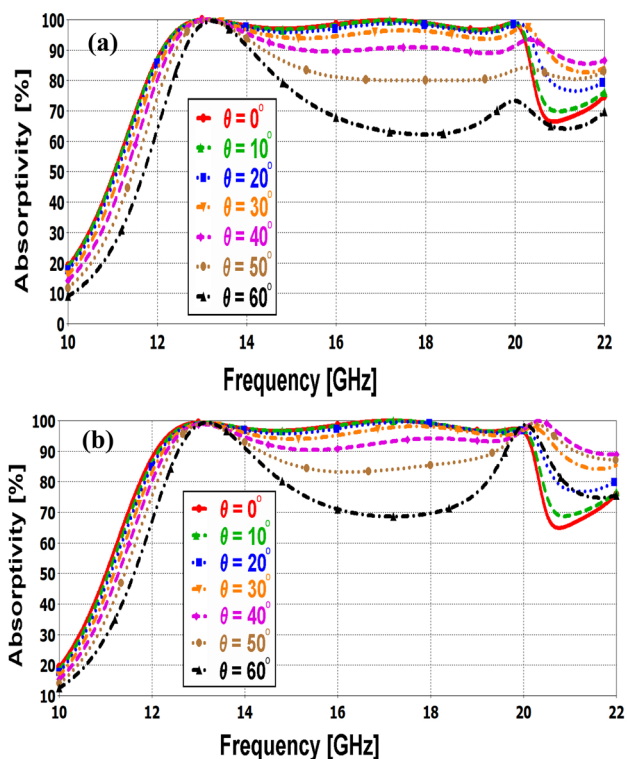


Fig. 4 The effect of the angle of incidence on the absorption response for **a** TE, **b** TM polarized modes

Fig. 5 Simulated electric fields (norm E) of the suggested PMMA at frequency of **a** 13 GHz, **b** 17.1 GHz, and at **c** 19.9 GHz

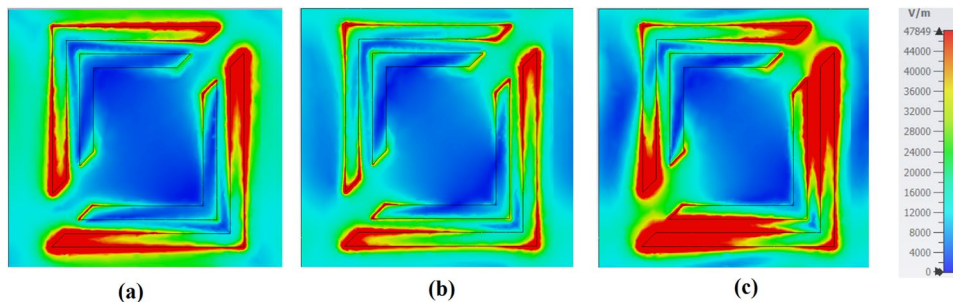
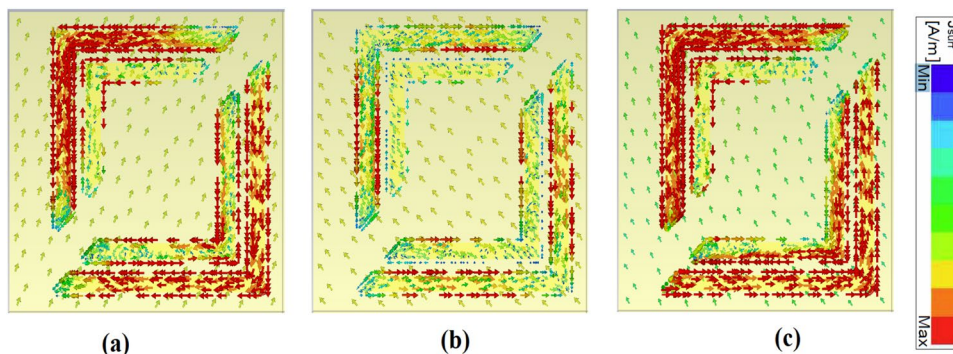


Fig. 6 Simulated surface current density of the suggested PMMA at frequency of **a** 13 GHz, **b** 17.1 GHz, and at **c** 19.9 GHz



(above 80% of absorptivity) for incidence angle variation up to 50° for both TE and TM polarizations as revealed from Fig. 4. In order to have better understanding of the absorption behavior of the suggested design, field distributions at three absorption peaks (13 GHz, 17.1 GHz, and 19.9 GHz with corresponding absorptivity of 99.9%, 99.9%, and 98.8%, respectively) are obtained and presented in Fig. 5. Figure 6 shows the corresponding surface current distributions at the same frequencies. It may be noted from Fig. 5 and Fig. 6 that the excited positive charges have been indicated by the red region, while the negative charges by blue region.

Due to the incident electromagnetic wave, the charges will oscillate resulting in electric resonance response. Electric dipoles have been excited due to positive and negative charges which explain the occurrence of the electric resonance response [16, 34]. Furthermore, at 19.9 GHz, strong field confinement is achieved through the L-shaped resonators where displacement currents are presented. This leads to magnetic resonance response [16].

Due to presence of both electric and magnetic resonance responses, a perfect and wideband absorber is presented. Equation (6) [35] can be used to illustrate the presence of both electric and magnetic resonance

that are required to obtain a perfect metamaterial absorber.

$$A = 1 - R = 1 - \left| \frac{Z - Z_0}{Z + Z_0} \right|^2 = 1 - \left| \frac{\sqrt{\mu_{eff}} - \sqrt{\epsilon_{eff}}}{\sqrt{\mu_{eff}} + \sqrt{\epsilon_{eff}}} \right|^2 \quad (6)$$

where Z is metamaterial impedance, Z_0 is the free space impedance while ϵ_{eff} and μ_{eff} are the frequency-dependent relative permittivity and permeability of the metamaterial. It may be seen from Eq. (6) that the perfect absorption is obtained as the impedance matching ($Z = Z_0$ or $\mu_{eff} = \epsilon_{eff}$) is achieved. It is worth noting that the impedance matching can be obtained by presence of both electric and magnetic resonances [35].

In order to better clarify the absorbing mechanism of the PMMA, the transmission line model can be used to simulate the suggested PMMA as previously reported in [14] and [16]. In this context, Nguyen and Lim [14] have proposed a broadband metamaterial absorber with absorption ratio higher than 90% through the frequency range 8.2–13.4 GHz. Further, a circuit model has been suggested with three series RLC connected in parallel in order to represent the three resonance absorption peaks at 9 GHz, 11 GHz and 13 GHz [14]. It worth noting that our suggested design has absorptivity above 90% over frequency range 12–20 GHz. Further, three resonance absorption peaks are obtained at 13 GHz, 17.1 GHz, and 19.9 GHz. Consequently, the transmission line model of the proposed PMMA shown in Fig. 7 is similar to that presented in [14]. The three series RLC branches connected in parallel are used to model the L-shaped resonators. However, L_d , R_d , Z_1 and Z_2 represent the dielectric substrate. Additionally, the continuous

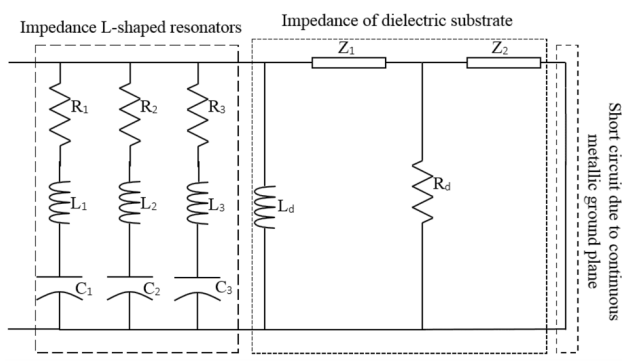


Fig. 7 Transmission line model for the suggested PMMA unit cell

metallic ground plane is described by a short circuit due to its perfect reflectivity. The circuit parameters shown in Fig. 7 are extracted as $R_1 = 20 \Omega$, $R_2 = 20 \Omega$, $R_3 = 1000 \Omega$, $L_1 = 69 \text{ nH}$, $L_2 = 20 \text{ nH}$, $L_3 = 100 \text{ nH}$, $C_1 = 0.9 \text{ fF}$, $C_2 = 7.3 \text{ fF}$, $C_3 = 20 \text{ fF}$, $L_d = 1.4 \text{ nH}$, $R_d = 55 \Omega$, $Z_1 = 50 \Omega$ with an electrical length 88° and $Z_2 = 50 \Omega$ with an electrical length 70° . The impedance of the proposed absorber (Z) should equal to the free space impedance (Z_0) over the operating frequency band to obtain perfect absorptivity as evident from Eq. (6). Figure 8 shows the absorption response of the suggested PMMA calculated by the FEM compared to that calculated using the extracted circuit model. It is evident that a good agreement is obtained between the two results which ensure the high accuracy of our suggested model.

The geometrical parameters are next studied to investigate their effects on both the absorptivity and absorption frequency band. Figure 9 shows the effect of the periodicity (a) of the unit cell on the absorptivity. In this study, the periodicity is varied from 3.4 mm to 4.4 mm while the other parameters are fixed at their initial values. It may be noticed from Fig. 9 that as the periodicity of the unit cell increases, the absorptivity increases while the absorption frequency band decreases. In order to achieve perfect and wideband absorber, the optimal value of the periodicity is taken as 3.7 mm. Next, the impact of the substrate thickness (h) is studied. Figure 10 shows the effect of the substrate thickness (h) on the absorptivity and absorption

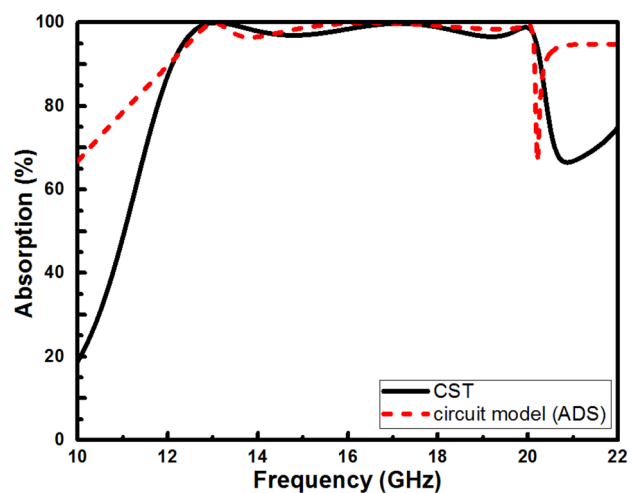


Fig. 8 Comparison between absorptivity calculated by CST and that calculated by circuit model for the suggested PMMA unit cell

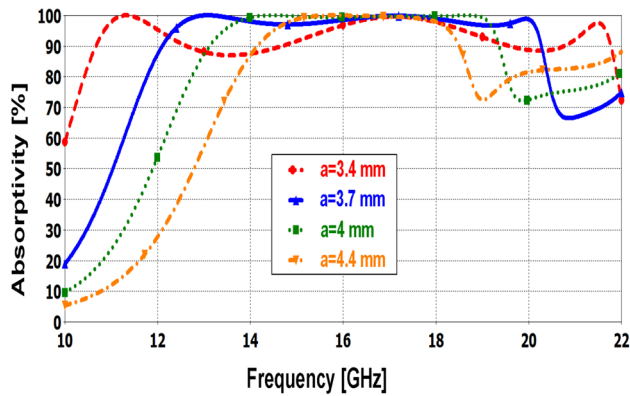


Fig. 9 Effect of the periodicity (a) of the unit cell on the absorptivity and absorption frequency band

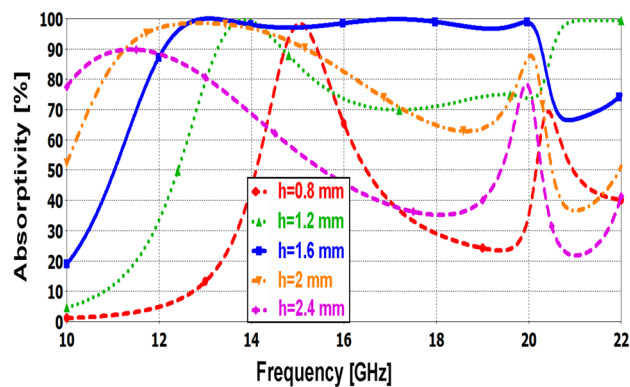


Fig. 10 Effect of the substrate thickness (h) on the absorptivity and absorption frequency band

band of the reported design. During this investigation, the substrate thickness is varied from 0.8 mm to 2.4 mm while the periodicity is fixed at 3.7 mm, and the other parameters are fixed at their initial values. As shown from Fig. 10, the substrate thickness has an important effect on the response of the absorption which can configure the absorber as wideband or multiple band absorber. The perfect absorptivity can be obtained by reducing the reflection coefficient Eq. (5). This can be achieved through matching impedance between the input impedance of the PMMA and the impedance of free space. It is worth noting that the substrate thickness has an effect on the real part of the input impedance [36] as shown from Eqs. (1, 2 and 6). Consequently, the optimal value of the substrate thickness that achieves a wideband and high absorptivity is 1.6 mm.

Figure 11 represents the effect of the separation (d) on the absorptivity. Through this study, the

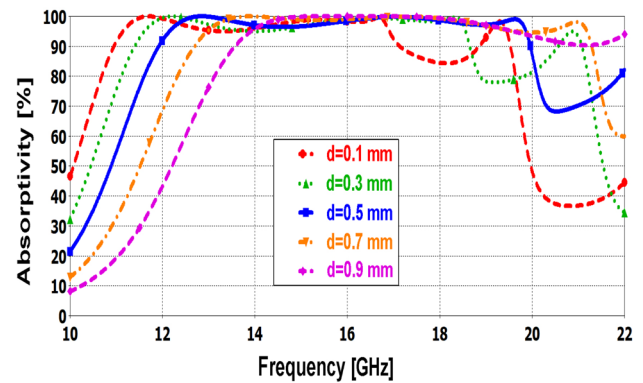


Fig. 11 Effect of the separation (d) on the absorptivity and absorption frequency band

periodicity and the substrate thickness are fixed at 3.7 mm, and 1.6 mm, respectively. However, the other parameters are fixed at their initial values. It may be seen from Fig. 11 that as the separation decreases, the absorption frequency band is shifted to left. This shift is a result to the equivalent parasitic capacitor between the two metallic resonators. As the separation (d) decreases, the parasitic capacitor decreases which reduces the operating frequency. Also, Fig. 11 shows that as the separation decreases, the wideband response of the absorption gradually tends to be dual band as the third resonance peak is separated from the wide absorption band. So, the optimal value is chosen equal to 0.5 mm.

It is worth noting that the effect of the remainder parameters are not investigated and chosen as initial values due to our fabrication limits. Table 1 shows the optimum values of the geometrical parameters.

In order to experimentally verify the performance of the proposed PMMA, a prototype is fabricated based on the optimum geometrical parameters using photolithography process. The fabricated prototype has dimensions of $148 \times 148 \times 1.6$ mm (40×40 unit cells) using copper coated FR-4 substrate on both sides with a copper thickness of 0.035 mm. Figure 12 shows the fabricated prototype with the measurement setup shown in Fig. 13. A horn antenna and a vector network analyzer (AgilentFieldFox® model N9918A) are used to measure the S-parameters of the proposed PMMA. First, the S-parameters of a perfect reflector (reference object) is measured. Then, the S-parameters of the proposed PMMA is obtained. Finally, the two sets of the measured data are subtracted to reduce

Table 1 The value of the optimized parameters of the proposed PMMA

| Parameter | h | a | G | p | w | d |
|------------|-----|-----|-----|-----|-----|-----|
| Value (mm) | 1.6 | 3.7 | 0.3 | 0.2 | 0.2 | 0.5 |

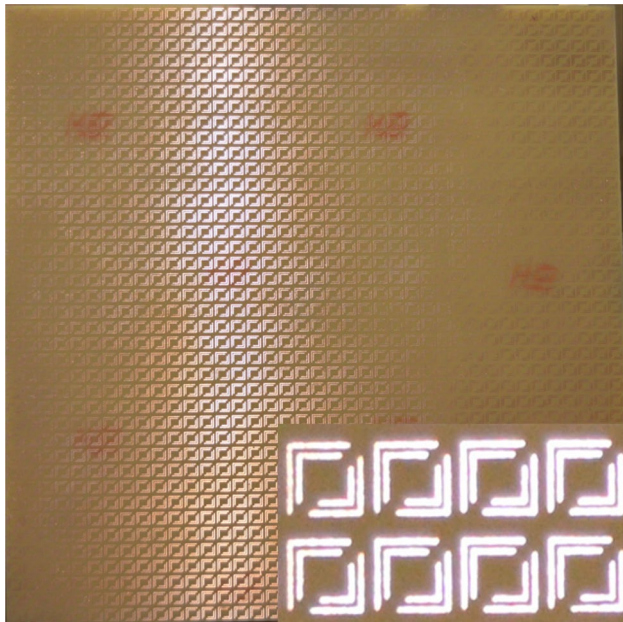


Fig. 12 Image of the fabricated PMMA

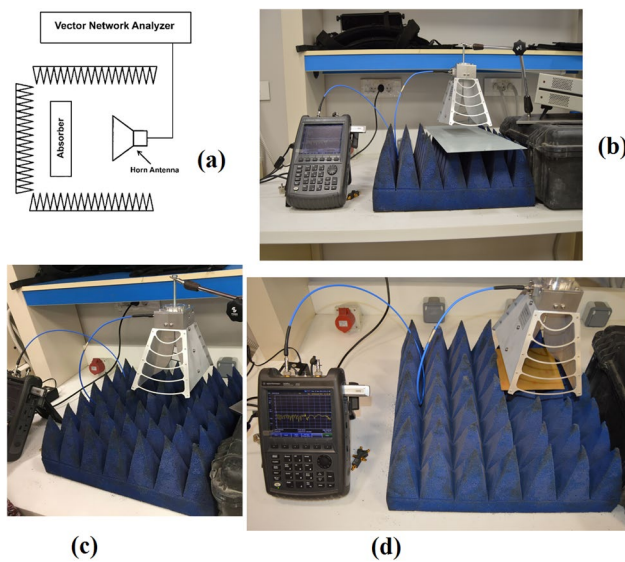


Fig. 13 **a** Schematic diagram of the measurement setup, **b** measurement of S-parameters for the perfect reflector (as a reference), **c** measurement of S-parameters for the pyramidal perfect absorber, and **d** measurement of S-parameters for the proposed PMMA

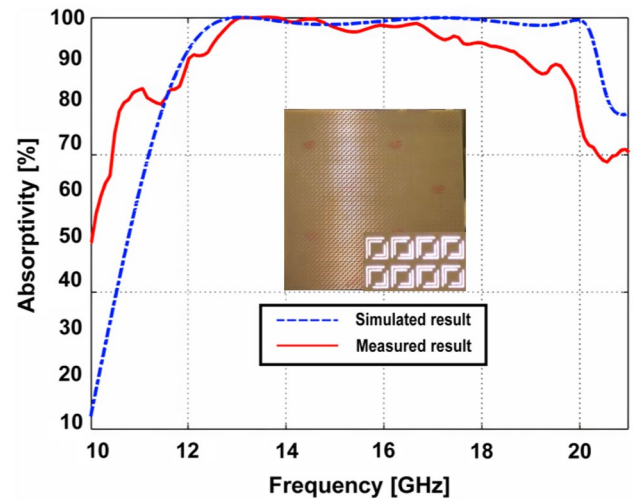


Fig. 14 Measured and simulated absorptivity of the proposed PMMA

the interference caused by many factors, such as edge reflection, diffraction loss, and scattering loss.

The measured absorption of the suggested PMMA is shown in Fig. 14 compared to the simulated results where a good agreement is achieved. It may be seen from Fig. 14 that the fabricated design has a smaller absorption than that of the simulated structure. Such a difference is due to the effect of the diffraction and scattering waves [26] where the geometry infinite conditions have not been achieved in the fabricated sample. Therefore, edge diffraction can occur during the characterization process. Further, slight variation may occur during the fabrication process. Additionally, the suggested PMMA can be improved by tuning the operating frequency band by adding an active element such as varactor diode [37]

The performance of the suggested PMMA is compared with the previously reported wideband metamaterial absorbers. Table 2 shows the comparison study of the performance metamaterial absorbers including the absorption bandwidth, unit cell dimension, substrate thickness, and maximum absorptivity. Table 2 also shows if the studied structures are based on multi-layered and lumped elements or not. It can be seen from Table 2 that the reported design of PMMA has many merits such as; small

Table 2 The performance of the reported structure relative to those reported in the literature

| Refs. | BW (GHz) | Unit cell dimension (mm) | Thickness (mm) | Maximum absorptivity (%) | Multi-layered/lumped elements |
|--|----------|--------------------------|----------------|--------------------------|-------------------------------|
| This work | 12–20.2 | 3.7×3.7 | 1.6 | 99.9 | No/No |
| Defected circle [15] | 8–18 | 9.7×9.7 | 2.5 | 99.4 | No/Yes |
| Metallic square spirals [16] | 11.4–20 | 3.65×3.65 | 1.6 | 99.8 | No/No |
| Multilayered square loops [21] | 5.2–18 | 13×13 | 4.8 | 97 | Yes/Yes |
| Artificial impedance surface [22] | 7.6–18.3 | 10×10 | 3.25 | 98.5 | Yes/Yes |
| metal ring and wire [38] | 2.5–10 | 20×20 | 9.9 | 99.8 | No/Yes |
| Double-square loops [39] | 8–18 | 13×13 | 3.175 | 95 | No/Yes |
| Lumped resistors loaded frequency selective surface [31] | 7.2–12.5 | 12.8×12.8 | 5.2 | 94.1 | Yes/Yes |

thickness, perfect absorptivity, wideband of absorption response without using multilayer or lumped elements.

4 Conclusion

A wideband, ultrathin and polarization insensitive perfect metamaterial absorber is proposed and investigated for Ku-band. The reported PMMA has absorptivity above 90% over wideband frequency range from 12 to 20.2 GHz for TE and TM polarizations. Also, the suggested design has high absorption response (above 80% of absorptivity) with incident angle variation (up to 50°) with a subwavelength unit cell (0.064λ). A prototype of the suggested PMMA (148×148 mm) is fabricated and characterized which shows a good agreement with the simulated results.

Author contributions

All authors certify that they have participated sufficiently in the work to take public responsibility for the content.

Funding

Open access funding provided by The Science, Technology & Innovation Funding Authority (STDF) in cooperation with The Egyptian Knowledge Bank

(EKB). The authors declare that no funds, grants, or other support were received during the preparation of this manuscript.

Data availability

The data will be available upon request.

Declarations

Competing interests The authors would like to clarify that there is no financial/non-financial interests that are directly or indirectly related to the work submitted for publication.

Open Access This article is licensed under a Creative Commons Attribution 4.0 International License, which permits use, sharing, adaptation, distribution and reproduction in any medium or format, as long as you give appropriate credit to the original author(s) and the source, provide a link to the Creative Commons licence, and indicate if changes were made. The images or other third party material in this article are included in the article's Creative Commons licence, unless indicated otherwise in a credit line to the material. If material is not included in the article's Creative Commons licence and your intended use is not permitted by statutory regulation or exceeds the permitted use, you will need to obtain permission di-

rectly from the copyright holder. To view a copy of this licence, visit <http://creativecommons.org/licenses/by/4.0/>.

References

1. N. Engheta, R.W. Ziolkowski (eds.), *Metamaterials: physics and engineering explorations* (John Wiley, Hoboken, 2006)
2. N. Garcia, M. Nieto-Vesperinas, Left-handed materials do not make a perfect lens. *Phys. Rev. Lett.* **88**(20), 207403 (2002)
3. W. Cai, U.K. Chettiar, A.V. Kildishev, V.M. Shalaev, Optical cloaking with metamaterials. *Nat. Photonics* **1**(4), 224–227 (2007)
4. F. Dincer, M. Karaaslan, E. Unal, O. Akgol, C. Sabah, Design of polarization-and incident angle-independent perfect metamaterial absorber with interference theory. *J. Electron. Mater.* **43**(11), 3949–3953 (2014)
5. M. Bağmancı, M. Karaaslan, E. Ünal, O. Akgol, C. Sabah, Extremely-broad band metamaterial absorber for solar energy harvesting based on star shaped resonator. *Opt. Quant. Electron.* **49**(7), 1–14 (2017)
6. C. Sabah, F. Dincer, M. Karaaslan, E. Unal, O. Akgol, E. Demirel, Perfect metamaterial absorber with polarization and incident angle independencies based on ring and cross-wire resonators for shielding and a sensor application. *Opt. Commun.* **322**, 137–142 (2014)
7. A.R.M. Ghanim, M. Hussein, M.F.O. Hameed, Highly directive hybrid Yagi-Uda nanoantenna for radiation emission enhancement. *IEEE Photonics J.* **8**, 1–12 (2016)
8. D. Schurig et al., Metamaterial electromagnetic cloak at microwave frequencies. *Science* **314**, 977–980 (2006)
9. M. Li, S.Q. Xiao, Y.Y. Bai, B.Z. Wang, An ultrathin and broadband radar absorber using resistive FSS. *IEEE Antennas Wirel. Propag. Lett.* **11**, 748–751 (2012)
10. M. Amiri, F. Tofigh, N. Shariati, J. Lipman, M. Abolhasan, Review on metamaterial perfect absorbers and their applications to IoT. *IEEE Internet Things J.* **8**(6), 4105–4131 (2020)
11. A.S. Saadeldin, M.F.O. Hameed, E.M. Elkaramany, S.S. Obayya, Highly sensitive terahertz metamaterial sensor. *IEEE Sens. J.* **19**(18), 7993–7999 (2019)
12. H. Xiong, J.S. Hong, C.M. Luo, L.L. Zhong, An ultrathin and broadband metamaterial absorber using multi-layer structures. *J. Appl. Phys.* **114**(6), 064109 (2013)
13. F. Ding, Y. Cui, X. Ge, Y. Jin, S. He, Ultra-broadband microwave metamaterial absorber. *Appl. Phys. Lett.* **100**(10), 103506 (2012). <https://doi.org/10.1063/1.3692178>
14. T.T. Nguyen, S. Lim, Design of metamaterial absorber using eight-resistive-arm cell for simultaneous broadband and wide-incidence-angle absorption. *Sci. Rep.* **8**(1), 1–10 (2018)
15. T.K.T. Nguyen, T.N. Cao, N.H. Nguyen, X.K. Bui, C.L. Truong, D.L. Vu, T.Q.H. Nguyen, Simple design of a wide-band and wide-angle insensitive metamaterial absorber using lumped resistors for X-and Ku-bands. *IEEE Photonics J.* **13**(3), 1–10 (2021)
16. J.B.O. De Araújo, G.L. Siqueira, E. Kemptner, M. Weber, C. Junqueira, M.M. Mosso, An ultrathin and ultrawideband metamaterial absorber and an equivalent-circuit parameter retrieval method. *IEEE Trans. Antennas Propag.* **68**(5), 3739–3746 (2020)
17. R.V. Jagtap, A.D. Ugale, P.S. Alegaonkar, Ferro-nano-carbon split ring resonators a bianisotropic metamaterial in X-band: constitutive parameters analysis. *Mater. Chem. Phys.* **205**, 366–375 (2018)
18. M.B. Hossain, M.R. Faruque, M.T. Islam, M. Singh, Jusoh M Triple band microwave metamaterial absorber based on double E-shaped symmetric split ring resonators for EMI shielding and stealth applications. *J. Mater. Res. Technol.* **18**, 1653–1668 (2022)
19. C.-S. Ri, H.-J. Yun, S.-J. Im, Y.-H. Han, Bandwidth analysis of microwave metamaterial absorber with a resistive frequency selective surface by using an equivalent circuit model. *AEU-Int. J. Electron. Commun.* **148**, 154160 (2022)
20. [online] CST Microwave Studio, (2021). [http:// www.cst.com](http://www.cst.com)
21. S. Ghosh, S. Bhattacharyya, K.V. Srivastava, Design, characterisation and fabrication of a broadband polarisation-insensitive multilayer circuit analogue absorber. *IET Microw. Antenna Propag.* **10**(8), 850–855 (2016)
22. M. Yoo, S. Lim, Polarization-independent and ultrawide band metamaterial absorber using a hexagonal artificial impedance surface and a resistor-capacitor layer. *IEEE Trans. Antennas Propag.* **62**(5), 2652–2658 (2014)
23. Y. Wu, S. Tan, Y. Zhao, L. Liang, M. Zhou, G. Ji, Broadband multispectral compatible absorbers for radar, infrared and visible stealth application. *Prog. Mater. Sci.* (2023). <https://doi.org/10.1016/j.pmatsci.2023.101088>
24. A. Sharma, R. Panwar, R. Khanna, Design and development of low radar cross section antenna using hybrid metamaterial absorber. *Microw. Opt. Technol. Lett.* **61**(11), 2491–2499 (2019)

25. P. Zuo, T. Li, M. Wang, H. Zheng, E.-P. Li, Miniaturized polarization insensitive metamaterial absorber applied on EMI suppression. *IEEE Access* **8**, 6583–6590 (2019)
26. O. Almirall, R. Fernández-García, I. Gil, Wearable metamaterial for electromagnetic radiation shielding. *J. Text. Inst.* **113**(8), 1586–1594 (2022)
27. D.Q. Vu, D.H. Le, H.T. Dinh, T.G. Trinh, L. Yue, D.T. Le, D.L. Vu, Broadening the absorption bandwidth of metamaterial absorber by coupling three dipole resonances. *Physica B* **532**, 90–94 (2018)
28. K.L. Zhang, Z.L. Hou, L.B. Kong, H.M. Fang, K.T. Zhan, Origin of negative imaginary part of effective permittivity of passive materials. *Chin. Phys. Lett.* **34**(9), 097701 (2017)
29. R.A. Sekar, S.R. Inabathini, An ultra-thin compact wideband metamaterial absorber. *Radioengineering*. **27**(2), 365 (2018)
30. C. Barde, A. Choubey, R. Sinha et al., A compact wideband metamaterial absorber for Ku band applications. *J Mater Sci: Mater Electron* **31**, 16898–16906 (2020). <https://doi.org/10.1007/s10854-020-04245-2>
31. H. Chen et al., Flexible and conformable broadband metamaterial absorber with wide-angle and polarization stability for radar application. *Mater. Res. Exp.* **5**, 015804 (2018)
32. Y.H. Jia, P. Gong, S.L. Li, W.D. Ma, X.Y. Fang, Y.Y. Yang, M.S. Cao, Effects of hydroxyl groups and hydrogen passivation on the structure, electrical and optical properties of silicon carbide nanowires. *Phys. Lett. A* **384**(4), 126106 (2020). <https://doi.org/10.1016/j.physleta.2019.126106>
33. Y.Y. Yang, P. Gong, W.D. Ma, R. Hao, X.Y. Fang, Effects of substitution of group-V atoms for carbon or silicon atoms on optical properties of silicon carbide nanotubes. *Chinese Phys. B* **30**(6), 067803 (2021). <https://doi.org/10.1088/1674-1056/abdb1e>
34. Y. Cheng, H. Zou, J. Yang, X. Mao, R. Gong, Dual and broadband terahertz metamaterial absorber based on a compact resonator structure. *Optical Mater. Exp.* **8**(10), 3104–3114 (2018)
35. W. Zhu, Electromagnetic metamaterial absorbers: from narrowband to broadband. *Metamater. Metasurfaces* (2018). <https://doi.org/10.5772/intechopen.78581>
36. F. Costa, S. Genovesi, A. Monorchio, G. Manara, A circuit-based model for the interpretation of perfect metamaterial absorbers. *IEEE Trans. Antennas Propag.* **61**(3), 1201–1209 (2012)
37. T. Wu, W. Li, S. Chen, J. Guan, Wideband frequency tunable metamaterial absorber by splicing multiple tuning ranges. *Results Phys.* **1**(20), 103753 (2021)
38. S. Fan, Y. Song, Ultra-wideband flexible absorber in microwave frequency band. *Materials* **13**(21), 4883 (2020)
39. J. Yang, Z. Shen, A thin and broadband absorber using double-square loops. *IEEE Antennas Wirel. Propag. Lett.* **6**, 388–391 (2007)

Publisher's Note Springer Nature remains neutral with regard to jurisdictional claims in published maps and institutional affiliations.